

The OH Masers Towards IRAS 19092 + 0841

K. A. Edris¹, G. A. Fuller², S. Etoka², and R. J. Cohen²

¹ Department of Astronomy and Meteorology, Faculty of science, Al-Azhar University, PO Box 11884, Naser City, Cairo, Egypt (e-mail: khedres@azhar.edu.eg)

² Jodrell Bank Centre for Astrophysics, School of Physics and Astronomy, Alan Turing Building University of Manchester, Manchester, M13 9PL, UK

the date of receipt and acceptance should be inserted later

Abstract. We present high angular resolution spectral line observations of ground state OH maser emission towards the young high mass proto-stellar object IRAS 19092+0841. The two OH main spectral lines, 1665 and 1667 MHz were observed using MERLIN. The two OH lines have been detected close to the central object. The interferometric data have been reduced and a map for both observed frequencies have been produced. The positions and velocities of the OH maser components have been determined. The polarization properties of the OH maser components were determined as well. The main components OH maser components are spread over a region of $\sim 5''$ corresponding to 22400 AU (or ~ 0.1 pc) at a distance 4.48 kpc. The spread of the relatively small velocity range of the OH masers over a relatively wide distribution and their association of the 44 GHz class I methanol masers indicate that the OH masers emission is probably associated with the external shell of a collapsing core. With the absence of any sign of a disk, outflow or an UCHII region, this would be the first OH masers associated with a star forming region in such an early evolutionary stage. High angular resolution observations of other tracers are needed to reveal the nature of this source. The association between OH masers and the two classes of methanol masers could be a crude evolutionary indicator, such that an association OH masers-class I methanol masers would indicate an earlier evolutionary state than the association OH masers-class II methanol masers. Surveys of class I and class II methanol masers towards OH masers sources are needed to confirm this suggestion.

Key words. stars: formation, masers, ISM: individual: IRAS 19092 + 0841

1. Introduction

OH masers observations show that they are associated with different evolutionary stages. It was believed that they are associated with only HII regions. However observations which have been carried out towards of a number of star forming regions show that OH masers are also associated with an earlier stage before the appearance of ionized HII regions (e.g. Cohen et al 1988; Braz et al. 1990). This type of OH maser is associated with an accretion phase, outflow, and circumstellar disks (Brebner et al. 1987; Hutawarakorn, & Cohen 1999; Hutawarakorn et al 2002; Fuller et al 2001; Edris et al. 2005). An OH maser survey by Edris, Fuller, & Cohen (2007, hereafter EFC07) detected the OH masers towards 26% towards a sample of 217 High Mass Protostellar Objects (HMPOs) candidates. It is of interest to know the distributions of the OH masers and their associations towards these regions in addition to their position in the evolutionary sequence. Maser emission gives a unique opportunity of observing those typically far regions in some details. This paper is

the first follow up of EFC07 survey with a high angular resolution observation. One of EFC07 objects (IRAS 20126+4104, hereafter IRAS20126) was studied by Edris et al. (2005) at the three masers types, OH, H₂O and class II CH₃OH masers.

The present object of study, IRAS 19092+0841 (hereafter IRAS19092), is one of the HMPOs sample studied by Molinari et al. (1996; 1998; 2000; 2002). Molinari et al (1996) so-called '*high & Low*' sources are a subsample from the Palla et al (1991) sample of 260 IRAS sources (basically candidates for compact molecular cloud association as defined by Richards et al. (1987)). *High* sources are the one located in the 'higher' part of the colour-colour diagram such that: $[25-12]_c=0.57$ (which in essence is the prescription for the presence of associated UCHII regions according to Wood & Churchwell 1989 criteria). On the other hand, '*Low*' sources are most probably made of 2 distinct evolutionary groups: a very 'early' one (before the creation of a 'real' YSO at the centre and consequently before the appearance of any measurable/detectable UCHII regions; and a more evolved group

Observational parameters	OH masers
Date of observation	4 & 5 April 2003
Antenna Used	seven antenna
Field centre (2000)	$\alpha 19^h 11^m 37.40^s$ $\delta 08^\circ 46' 30.00''$
Rest frequency (MHz)	1665.402 1667.359
No. of frequency channels	512
Total bandwidth (MHz)	0.5
bandpass calibrator	3C84
Polarization angle calibrator	3C286
Phase calibrator	1919+086

Table 1. Observing and calibration parameters for the MERLIN spectral-line observations of IRAS 19092+0841

(older than the 'High sources group' containing objects which have already dispersed much of their circumstellar material. And, IRAS19092 belongs to the latter category. IRAS19092 is at an estimated distance of 4.48 kpc (Molinari et al. 1996) and has a luminosity of $9200 L_\odot$ (Molinari et al. 2002). An ammonia core was found towards IRAS19092 at velocity $\sim 58 \text{ km s}^{-1}$ (Molinari et al. 1996). Although IRAS19092 is a *Low* type Object, it is one of the few sources associated with different types of maser emission.

Water maser was detected by Brand et al. (1994) and Palla et al. (1991). Class II and class I CH_3OH masers were detected by Szymczak et al. (2000), Kurtz et al. (2004) and recently Fontani et al (2010). OH maser was originally reported by MacLeod et al. (1998). CO and H_2 observations failed to detect any outflows from this region (Zhang et al. 2005; Varricatt et al. 2010). It is not associated with a close radio continuum emission as well. The closest radio emission detected by Molinari et al. (1998) at 6 cm is offset from the IRAS position by 110 arcsec.

To determine what the OH masers trace and how they are distributed and related to other tracers, IRAS19092 have been observed at high angular resolution using MERLIN. The details of the observations and reduction are given in Sec. 2 and the results presented in Sec. 3. In Sec. 4 we discuss the interpretation while conclusions are drawn in Sec. 5.

2. Observations and data reduction

Table 1 gives the parameters for the MERLIN observations. The phase calibrator source 1919+086 was used to retrieve the absolute position of the maser spots and therefore compare their locations from one line to another. The absolute position accuracy of 37 mas was estimated following the procedures described in Edris et al. (2005). This positional uncertainty depends on four factors, the position accuracy of the phase calibrator, the accuracy of the telescope positions, the relative position error depending on the beamsize and signal-to-noise ratio and finally the atmospheric variability. A bandpass calibrator 3C84 was observed to calibrate the variation of instrumental

gain and phase across the spectral bandpass. Observations of 3C286 were also made during the observing run, with the same correlator configuration and bandwidth, to calibrate for the polarization angle. The data were initially reduced in Jodrell Bank observatory using the MERLIN d-programs and then the AIPS software package was used to complete the data reduction and produce the maps.

IRAS 19092+0841 was observed in the 1665- and 1667-MHz OH maser transitions in April 2003 using the seven telescopes of the MERLIN network available then. During the observations, the frequency was cycled between the two OH line frequencies, to provide data on both transitions spread over the whole observing track. The velocity resolution was 0.21 km s^{-1} for a total of 0.25 MHz spectrum bandwidth corresponding to 45 km s^{-1} velocity range. The left- and right-hand circular (LHC and RHC) polarization data for each baseline were simultaneously correlated in order to obtain all the Stokes parameters. Using the d-programs (see Diamond et al. 2003), the data were edited and corrected for gain-elevation effects. The flux density of the amplitude calibrator 3C84, was determined by comparing the visibility amplitudes on the shortest baselines with those of 3C286. Using flux density of 13.625 Jy for 3C286 (Baars et al. 1977), the flux density of 3C84 at the time of the observation was determined to be 21 Jy .

In AIPS the data were calibrated for all remaining instrumental and atmospheric effects. Starting from a point source model, the phase calibrator source was mapped, with a total of three rounds of phase self-calibration and the resulting corrections applied to the source data. The polarization leakage for each antenna was determined using 3C84 and the polarization position angle correction was performed using 3C286. The AIPS task IMAGR was used to map the whole data set in Stokes I, Q, U and V in order to retrieve the polarization information. The rms noise, after CLEANing, was typically 14 mJy/beam and the FWHM of the restoring beam is $0.9 \times 0.4 \text{ arcsec}$ at a position angle of -31° .

The positions of the maser components were determined by fitting two-dimensional Gaussian components to the brightest peaks in each channel map. Components were considered as spectral features if they occurred in three or more consecutive channels. Using flux weighted means over those channels of each group, the positions and velocities of spectrum features were obtained. The uncertainties in relative positions are typically 10 mas.

3. Results

The 1665- and 1667-MHz OH maser lines were detected with MERLIN. The absolute positions of brightest maser spot of the 1665 MHz OH line is at $19^h 11^m 38.974^s + 08^\circ 46' 31.09''$ at velocity 58 km s^{-1} .

A total of 11 (9 at 1665-MHz line and 2 at 1667-MHz line) OH maser spots were detected. At the 1665-MHz line, there are 5 left hand circular polarisation (LHC) and 4 right hand circular polarisation (RHC) components while

No.	Vel. km s ⁻¹	Flux Jy/b	RA h m s	Error s	DEC ° ' "	Error "	Notes
1665-MHz LHC comp.							
1	60.65	0.17 ± 0.01	19 11 39.002	0.004	8 46 30.38	0.12	z1 -4.3 mG
2	60.59	0.77 ± 0.01	19 11 38.973	0.000	8 46 31.10	0.01	
3	60.70	0.05 ± 0.01	19 11 38.899	0.008	8 46 28.33	0.18	
4	60.58	0.18 ± 0.01	19 11 38.943	0.001	8 46 27.68	0.03	
5	60.50	0.10 ± 0.01	19 11 38.909	0.003	8 46 44.80	0.06	
RHC comp.							
6	57.98	0.48 ± 0.02	19 11 39.001	0.003	8 46 30.44	0.07	z1 -4.3 mG
7	58.08	1.53 ± 0.02	19 11 38.974	0.000	8 46 31.09	0.00	
8	58.07	0.14 ± 0.02	19 11 38.941	0.006	8 46 27.95	0.15	
9	58.09	0.25 ± 0.02	19 11 38.950	0.001	8 46 27.59	0.02	
1667-MHz LHC comp.							
1	60.67	0.48 ± 0.01	19 11 38.950	0.001	8 46 27.81	0.03	
2	60.55	0.40 ± 0.01	19 11 38.944	0.002	8 46 27.66	0.04	

Table 2. The parameters of the left and right hand circular polarisation components of 1665-MHz and the 1667-MHz OH masers detected towards IRAS 19092 + 0841. The label Z marks a Zeeman pair.

No.	Vel. km s ⁻¹	I Jy/b	Q Jy/b	U Jy/b	V Jy/b	P Jy/b	χ °	m _L %	m _C %	m _T %
1665-MHz										
1	60.65	0.05	0.00	0.02	-0.04	0.00	0.00	0.0	-81.4	81.4
2	60.59	0.44	0.04	0.07	-0.32	0.08	0.54	18.1	-71.2	73.5
3	60.70	0.04	0.00	0.00	0.00	0.00	0.00	0.0	0.0	0.0
4	60.58	0.11	0.00	0.00	-0.05	0.00	0.00	0.0	-45.3	45.3
5	60.50	0.05	0.00	0.00	0.00	0.00	0.00	0.0	0.0	0.0
6	57.98	0.12	0.00	-0.08	0.09	0.08	0.00	65.6	74.0	98.9
7	58.08	1.23	-0.12	-0.71	0.47	0.72	0.70	58.3	38.5	69.8
8	58.07	0.07	0.00	-0.05	0.05	0.05	-0.03	69.9	61.7	93.2
9	58.09	0.22	-0.03	-0.15	0.07	0.16	0.68	70.1	31.3	76.8
1667-MHz										
1	60.67	0.12	0.03	0.00	0.03	0.03	0.00	29.7	29.9	42.1
2	60.55	0.12	0.03	0.03	0.00	0.04	0.41	38.7	0.0	38.7

Table 3. The Stokes and polarisation parameters of the 1665- and 1667-MHz OH masers components detected towards IRAS 19092 + 0841.

the two components detected at the 1667-MHz line are LHC. Table 2 presents the parameters of the OH maser components detected, namely the velocities, peak intensities and positions for each hand of circular polarisation. The label Z marks a left-hand and right-hand polarised pair of components which originate at the same location and are identified as a Zeeman pair with a splitting of 2.5 km s⁻¹. Figure 1 shows the distribution of the OH maser spots. The OH maser spots are spread over a region of $\sim 5''$ corresponding to 22400 AU (or ~ 0.1 pc) at a distance 4.48 kpc. At the 1665-MHz line, there are two main features while at the 1667-MHz line, there is only one main feature. the bottom feature at the 1665-MHz line (relatively weaker than the top one) are consistent with the feature of the 1667-MHz line.

Table 3 presents the Stokes parameters I, Q, U and V, the polarisation position angle (χ) (angles are measured from N towards E), the linearly polarised flux P, the percentage of linear polarisation m_L , the percentage

of circular polarisation m_C and the total percentage of polarisation m_T of each feature. The Stokes intensities are shown as zero in this table if their flux is below the noise level. There are two spots are not polarised. All the RHC of the 1665-MHz and the 1667-MHz components are elliptically polarised.

4. Discussion

4.1. Comparison with Other tracers

The OH masers were previously detected by Macleod et al. (1998) and EFC07. There is no remarkable change between the three observations in the spectrum, velocity range or peak velocity but the flux density was stronger in the later survey. The flux density in the present observations is the weakest. Also in the survey of EFC07 the 1665 MHz (LHC) spectrum showed a weak feature at velocity 55 km s⁻¹ which did not appear in the spec-

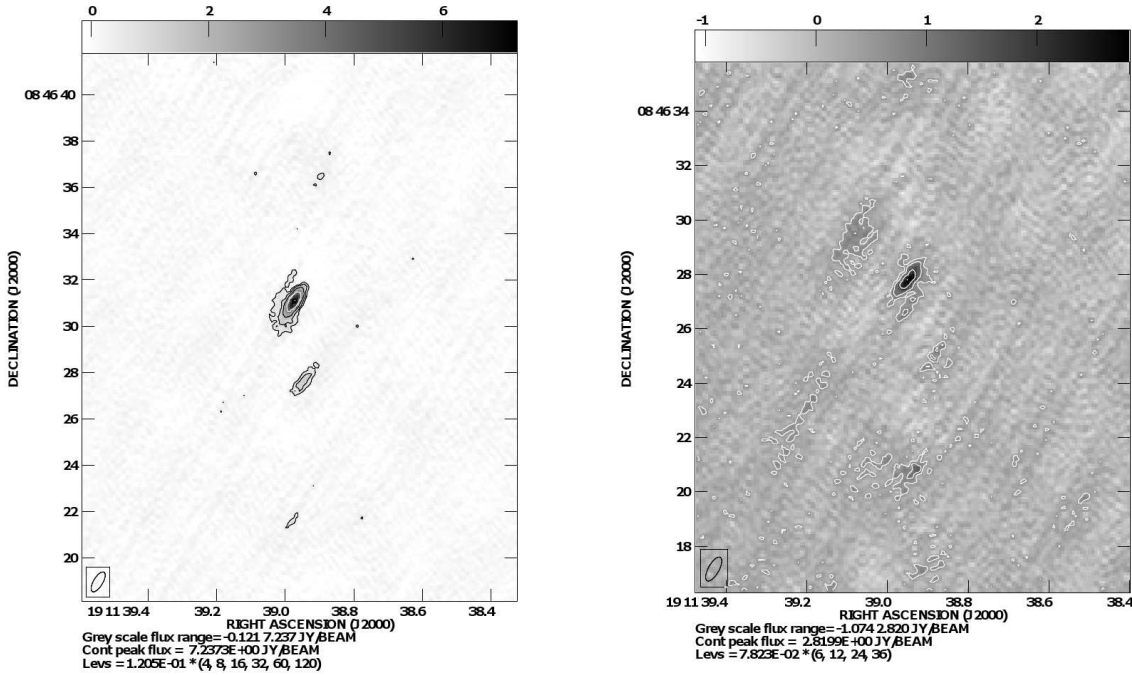


Fig. 1. The map of the 1665-(left) and 1667-MHz (right) OH maser emission from IRAS 19092+0841. The OH masers peak flux and contour levels are shown in the bottom of the map.

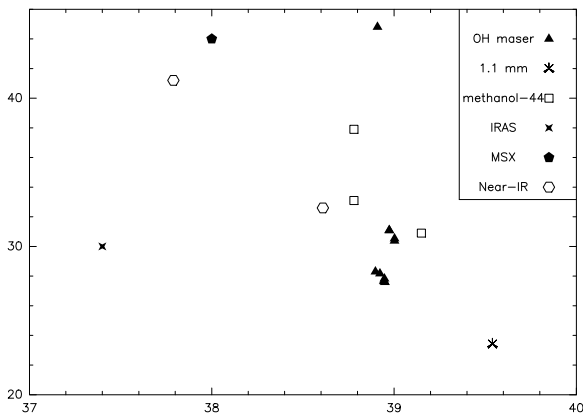


Fig. 2. The position of the OH maser spots, VLA class I Methanol maser spots from Kurtz et al. (2004), the closest 1.1 mm position (from BGPS survey, IRSA website), IRAS, MSX, and the K-band near-IR of 2MASS objects. The sign which refers to each tracer is shown in the upper right corner of the plot. The x- and y-axis is the right ascension in seconds of time and declination in arcsec of the leading terms α (2000) = 19^h 11m and δ (2000) = 08° 46' respectively. Note the close association between the OH masers and some 44-GHz Methanol maser spots.

trum of Macleod et al. (1998) or in this observation. This disappeared feature has the same velocity of the class

II methanol masers component at 6.7 GHz detected by Macleod et al. (1998), Szymczak et al. (2000), and more recently by Fontani et al. (2010). This OH feature may be associated with the class II methanol masers (which is more common in star forming regions). In the 6.7 GHz spectrum of Fontani et al. (2010) a new weaker methanol maser feature appears at velocity $\simeq 63 \text{ km s}^{-1}$ (their figure A-2).

IRAS19092 is associated with 44-GHz class I methanol masers but not with any 95-GHz class I methanol maser emission (Kurtz, Hofner, & Alvarez 2004; Fontani et al. 2010). The velocities of the OH maser components are consistent with those of the 44 GHz class I methanol masers. On the other hand, the 6.7 GHz class II methanol maser emission (centred at $V \sim 55 \text{ km s}^{-1}$) do not coincide with any OH maser spectral components; the separation with the closest OH maser components being of about 4–5 km s^{-1} . In addition, the positions of the 44 GHz spots (imaged by Kurtz, Hofner, & Alvarez 2004) at arcsec resolution using the VLA are closely associated with the OH masers spots (figure 2) while there is no high resolution observations at the 6.7 GHz to compare. The close association of OH (in particular the 1665 MHz line) and class II methanol masers have been proposed by Caswell (1996) from subarcsec accuracy survey and modeled by Cragg, Sobolev, & Godfrey. (2002). In some cases a disk has been suggested to be the source of the two maser types (Edris et al. 2005). However, a close association between OH masers and class I methanol masers towards

sources in such early (or indeed any) evolutionary state has never been reported so far. The flux ratio of these masers, $S(6668)/S(1665) = 6/1.5 = 4$ and $S(44)/S(1.6) = 1/1.5 = 0.6$, places IRAS19092 in OH-favoured sources. Note that although the OH and class I CH_3OH masers are associated, there is a clear difference in position, amounting to 2.7 arcsec (~ 0.06 pc), suggesting that the OH and CH_3OH masers are not co-propagating.

The water masers associated with IRAS19092 (Palla et al. 1991; Brand et al. 1994) peak at velocity $\simeq 57$ km s^{-1} with a velocity range of 2.5 km s^{-1} . This may indicate a more compact region than that of the OH masers.

The velocity of the strongest OH maser spot agrees with the gas velocity of the ammonia core measured by Molinari et al. (1996) as well as the peak velocity of the C^{34}S observations (which assumed to represent the velocity of the high-density gas) carried out by Brand et al. (2001). This indicates that the OH masers emission originated from the core of this region which is also consistent with the K_s object and submm map of Faustini et al (2009). The OH masers seem to arise from the core of the 850 μm and coincident with the K_s component. However the relatively small velocity spread of the OH maser spots despite their relatively large distributions (5'' or 17'' if the far northern component [1665-MHz C5] is included) indicates that the maser emission arises from material which is not close to the central object. The relatively small velocity spread may also refer to weak angular momentum and collapsing. This also indicates that the OH maser emission arises from material which is not very close to the central object. This is consistent with the relatively weak excitation temperature (10 K) compared to the gas kinetic temperature (40 K) (Fontani et al. 2006 and references therein). Measuring the deuterium fractionation and the CO depletion factor of IRAS19092 among 10 high-mass protostellar candidates, Fontani et al. (2006) proposed two scenarios for the location of emitting gas: 1) the cold gas is distributed in an external shell not yet heated up by the high-mass protostellar object, a remnant of the parental massive starless core. 2) the cold gas is located in cold and dense cores close to the high-mass protostar but not associated with it. The observations presented here support the first scenario mentioned. This also consistent with the association of the OH masers with the class I methanol masers at 44-GHz detected by Kurtz, Hofner, & Alvarez (2004). If the second scenario is true then the driving source needs still to be identified. Potential candidates are the two faint near-IR sources (detected in the 2MASS K-Band survey) and a mm sources (detect by the The Bolocam Galactic Plane Survey (BGPS) is a 1.1 mm, figure 2). Unfortunately, the poor positional uncertainty of these tracers does not allow us to draw any conclusion.

It is unclear whether the water and class II methanol masers at 6.7 MHz and indeed the IRAS and MSX source are associated with another source (may be consist with the other object to the north in the 2MASS [figure 2]) or associated with the driving source. The peak velocities

and velocity ranges of these other maser types are slightly different from that of OH masers. The water maser emission peak is centred at $V = 57.32$ km s^{-1} according to Palla et al. (2001, with a channel reso. of 0.66 km s^{-1}). This indicates that it is likely not tracing the same regions as the OH maser emission. The position of the IRAS and MSX is offset from the OH masers by $\simeq 0.5$ pc. High angular resolution observations of these tracers are needed to detect their positions and what they are trace.

4.2. Comparison with IRAS20126

IRAS20126 has been mapped at same high angular resolutions by Edris et al. (2005) in the ground-state lines of OH masers as well as the 22-GHz H_2O and the 6.7-GHz (class II) CH_3OH masers. When comparing the velocity range of the OH masers of IRAS19092 with that of IRAS20126, It is clear that towards the later the velocity range (~ 17 km s^{-1}) spread much more than that of the former (~ 3 km s^{-1}) although the spatial distributions of maser components work oppositely. The OH maser spots of IRAS19092 trace an area of angular size three times that of IRAS20126. The OH masers in IRAS20126 trace the circumstellar disk while there is no signature of a circumstellar disk towards IRAS19092. The strength of the magnetic field measured by a Zeeman pair in IRAS20126 is approximately 3 times stronger than that of IRAS19092. This indicates that IRAS19092 is in an earlier evolutionary stage than that of IRAS20126 which is consistent with the above indication (see Section 4.1). This also consists with the classification of Molinari et al. (1996). They classify IRAS19092 as a source from the *Low* sample while IRAS20126 belongs to the *High* sample.

The association of OH masers and the two classes of methanol masers are common between these two sources but at different spatial preferences. IRAS19092 is closely associated with class I while IRAS20126 is closely associated with class II (Edris et al. 2005). This can be confirmed in the case of IRAS20126 where there are high resolution observations at the two methanol classes. The class I 44 GHz methanol masers imaged in arcsec resolution using VLA by Kurtz et al. (2004) is ~ 7 arcsec ($\simeq 0.05$ pc) away from the OH maser position while the class II 6.7 GHz methanol masers is just $\simeq 0.1$ arcsec ($\simeq 0.001$ pc or 170 AU) away. Towards IRAS19092, there is only high resolution observations for class I 44 GHz methanol masers by also Kurtz et al. (2004) and the closest spot is $\simeq 0.2$ arcsec (0.004 pc) away from the OH masers. High resolution observations of 6.7 GHz methanol masers is needed to find out their association and confirm or reject the evolutionary indicator mentioned in section 4.3.

Towards IRAS20126, the flux density of the OH masers are stronger than that of IRAS19092. Also the strength of IRAS20126 magnetic field is approximately triple that of IRAS19092. Only the 1665-MHz OH line has been detected towards IRAS20126 while the 1665- and 1667-MHz lines have been detected towards IRAS19092. The pres-

ence of the two OH mainlines towards IRAS19092 indicates lower gas temperatures and lower density as predicted by the models of Cragg et al. (2002) and Gray et al (1991).

4.3. The Evolutionary Stage

The velocity spread and distribution of the OH masers indicate that collapse is the dominant process in that region. This suggests that this source is in a very early evolutionary state. This is consistent with the lack of deuterium reported by Fontani et al. (2006). These authors studied IRAS19092 among a sample of 10 high-mass protostellar candidates observed in two rotational molecular lines of N_2H^+ and N_2D^+ and the sub-millimeter continuum (850 μm). They concluded that IRAS 19092+0841 is associated with a cold and dense gas with chemical and physical conditions identical to those associated with low mass starless cores. This finding is also supported by the association of OH masers and class I methanol masers. Ellingsen (2006) suggested that the class I methanol masers may signpost an earlier stage of high-mass star formation than the class II masers. However Voronkov et al. (2010) suggest that sources associated with class I could be in more evolved evolutionary state, associated with an expanding HII region. And, in this stage, OH maser association is also expected. On the other hand, the lack of cm continuum emission and outflow signature (Molinari et al. 1998; Zhang et al. 2005; Watson et al. 2010) in addition to the weak flux density of the detected OH masers, suggests that IRAS19092 is in an earlier evolutionary state. The survey of EFC07 found that most of the detected sources show OH flux densities < 4.5 Jy, while the OH masers associated with HII regions show much higher flux densities (e.g. Gaume, & Mutel 1987; Gasiprong, Cohen, & Hutawarakorn 2002). The early evolutionary stage interpretation is also consistent with the suggestion of Molinari et al (1996) that the sources of the *Low* sample (which this source belongs to) are in an earlier evolutionary state than their *High* sample sources. The association between the OH masers and the class I and class II methanol masers could be used as a crude evolutionary indicator of the source with the association with the first indicating an earlier evolutionary state than the association with the later (see also Section 4.1).

The model of Cragg et al. (2002) can be used to place some constraints on the physical conditions. The presence of the 1667 MHz line as well as the 1665 MHz line indicates low gas temperatures and slightly lower brightness temperature. The specific column density $N/\Delta V$ is $< 10^{11.7}$ cm^{-1} s, where N is the column density of the OH maser molecule and ΔV is the linewidth.

5. Conclusions

Ground state OH maser emission at 1665 and 1667 MHz was observed towards IRAS19092 at high angular resolution using MERLIN. The OH maser spots are spread over

a region of $\sim 5''$ corresponding to 22400 AU (or ~ 0.1 pc) at a distance 4.48 kpc. We identify one Zeeman pair of OH masers and the splitting of this pair indicates a magnetic field of strength ~ 4.3 mG. The velocity range of the OH maser emission suggests that this source is in a collapsing state and the masers arise from the external shell of the collapsing core. With the absence of any sign of disk, outflow or HII region, this would be the first OH masers to be associated with a star forming region in such an early evolutionary stage.

The results of this paper suggest a close association between the OH masers and 44-GHz class I methanol masers in early evolutionary stage. The association between the OH masers and the two classes of the methanol masers could be used as a crude evolutionary indicator with the close association between the OH masers and class I indicates an earlier evolutionary state than its association with class II.

ACKNOWLEDGMENTS

MERLIN is a national facility operated by the University of Manchester at Jodrell Bank Observatory on behalf of PPARC.

References

- Brand, J., Cesaroni, R., Caselli, P., et al. 1994, A&AS, 103, 541
- Brand, J., Cesaroni, R., Palla, F., Molinari, S. 2001, A&A 370, 230
- Braz, M.A., Lepine, L.R.D., Sivagnanam, P., Le Squeren, A.M. 1990, A&A, 236, 479
- Brebner, G.C., Heaton, B., Cohen, R.J., Davies, S.R. 1987, MNRAS, 229, 679
- Caswell, J. L. 1996, MNRAS, 279, 79
- Cohen, R. J., Baart, E. E., Jonas, J. L. 1988, MNRAS, 231, 205
- Cragg, D. M., Sobolev, A. M., Godfrey, P. D. 2002, MNRAS, 331, 521
- Edris, K.A., Fuller, G.A., Cohen, R.J., Etoke, S. 2005, A&A, 343, 213
- Edris, K.A., Fuller, G.A., Cohen, R.J. 2007, A&A, 465, 865, EFC07
- Ellingsen, S.P., 2006, ApJ, 638, 241
- Faustini, F., Molinari, S., Testi, L., Brand, J. 2009, A&A, 503, 801
- Fontani, F., Caselli, P., Crapsi, A., et al. 2006, A&A, 460, 709
- Fontani, F., Cesaroni, R., Furuya, R.S. 2010, A&A, 517, 56
- Fuller, G.A., Zijlstra, A.A., Williams, S.J. 2001, ApJ, 555, L125
- Gasiprong, N., Cohen, R.J., Hutawarakorn, B. 2002, MNRAS, 336, 47
- Gaume, R.A., Mutel, R.L. 1987, ApJSS, 65, 193
- Gray, M.D., Doel, R.C., Field, D. 1991, MNRAS, 252, 30

- Hutawarakorn, B., Cohen, R. J. 1999, MNRAS, 303, 845
- Hutawarakorn, B., Cohen, R. J., Brebner, G. C. 2002, MNRAS, 330, 349
- Kurtz, S., Hofner, P., Alvarez, C.V. 2004, ApJSS, 155, 149
- MacLeod G., van der Walt D.J., North A., et al. 1998, AJ, 116, 2936
- Molinari, S., Brand, J., Cesaroni, R., Palla, F. 1996, A&A, 308, 573
- Molinari, S., Brand, J., Cesaroni, R., et al. 1998, A&A, 336, 339
- Molinari, S., Brand, J., Cesaroni, R., Palla, F. 2000, A&A, 355, 617
- Molinari, S., Testi, L., Rodríguez, L., Zhang, Q. 2002, ApJ 570, 758-778
- Palla, F., Brand, J., Cesaroni, R., et al. 1991, A&A, 246, 249
- Richards, P.J., Little, L.T., Toriseva, M., Heaton, B.D. 1987, MNRAS 228, 43
- Rosolowsky, E., Dunham, M.K., Ginsburg, A., et al. 2010, ApJS, 188, 123
- Szymczak, M., Hrynek, G., & Kus, A.J. 2000, A&AS, 143, 269
- Varricatt, W.P., Davis, C.J., Ramsay, S., Todd, S.P. 2010, MNRAS, 404, 661
- Voronkov, M.A., Caswell, J.L., Ellingsen, S.P., Sobolev, A.M. 2010, MNRAS, 405, 2471
- Zhang, Q., Hunter, T. R., Brand, J., et al. 2005, ApJ, 625, 864